On the Feasibility of Poisoning Text-to-Image AI Models via Adversarial Mislabeling

Stanley Wu
University of Chicago
Chicago, IL, USA
stanleywu@cs.uchicago.edu

Ronik Bhaskar
University of Chicago
Chicago, IL, USA
rbhaskar@cs.uchicago.edu

Anna Yoo Jeong Ha
University of Chicago
Chicago, IL, USA
annaha@cs.uchicago.edu

Shawn Shan
University of Chicago
Chicago, IL, USA
shawnshan@cs.uchicago.edu

Haitao Zheng
University of Chicago
Chicago, IL, USA
htzheng@cs.uchicago.edu

Ben Y. Zhao
University of Chicago
Chicago, IL, USA
ravenben@cs.uchicago.edu

Abstract

Today's text-to-image generative models are trained on millions of images sourced from the Internet, each paired with a detailed caption produced by Vision-Language Models (VLMs). This part of the training pipeline is critical for supplying the models with large volumes of high-quality image-caption pairs during training. However, recent work suggests that VLMs are vulnerable to stealthy adversarial attacks, where adversarial perturbations are added to images to mislead the VLMs into producing incorrect captions.

In this paper, we explore the feasibility of adversarial mislabeling attacks on VLMs as a mechanism to poisoning training pipelines for text-to-image models. Our experiments demonstrate that VLMs are highly vulnerable to adversarial perturbations, allowing attackers to produce benign-looking images that are consistently miscaptioned by the VLM models. This has the effect of injecting strong "dirty-label" poison samples into the training pipeline for text-to-image models, successfully altering their behavior with a small number of poisoned samples. We find that while potential defenses can be effective, they can be targeted and circumvented by adaptive attackers. This suggests a cat-and-mouse game that is likely to reduce the quality of training data and increase the cost of text-to-image model development. Finally, we demonstrate the real-world effectiveness of these attacks, achieving high attack success (over 73%) even in black-box scenarios against commercial VLMs (Google Vertex AI and Microsoft Azure).

CCS Concepts

• **Computing methodologies → Machine learning**; **Artificial intelligence**; • **Security and privacy**;

Keywords

Text-to-Image Diffusion Models; Data Poisoning Attacks; Adversarial Perturbations; Vision Language Models

1 Introduction

Today's generative text-to-image models [5, 50, 57, 70] are trained on massive datasets containing millions of images scraped from online sources, and new images are continuously scraped to train future updates. Increasingly, model trainers rely on Vision-Language Models (VLMs) [40, 76, 84] to generate detailed captions for scraped images. This labeling process is a significant improvement over HTML alt-text captions [44, 61] and creates accurate image-caption pairs critical to the model training pipeline.

However, recent work shows that VLMs are vulnerable to attacks, where imperceptible adversarial perturbations added to an image will manipulate VLMs into producing incorrect or misleading captions [25, 83, 92]. Similar to adversarial examples for DNN classifiers, these attacks can be "targeted," i.e., an attacker can compute perturbations for a given image that induces a VLM model to output a specific caption.

Given the pivotal role of VLMs in labeling training data for generative image models, their vulnerability can have significant downstream implications. In particular, we ask the question, "does the susceptibility of VLMs to mislabeling attacks create a new attack vector against generative text-to-image models?" In other words, could an attacker modify benign images in imperceptible ways such that when processed by VLMs, they produce incorrect labels, resulting in a mislabeled image-caption pair that performs the equivalent of a "dirty-label" poison attack on the model training process? We refer to this as an *adversarial mislabeling poison* attack, or AMP for short. We show an example in Figure 1.

In this paper, we perform a detailed study to determine if AMP attacks are indeed feasible today, and to understand their potential impact on real-world generative image models. *First*, we survey existing documentation on text-to-image models to gauge their reliance on VLMs for generating image captions. *Second*, we implement a targeted adversarial mislabeling poison attack, and experimentally measure its efficacy on multiple popular open-source VLMs with diverse architectures and operating parameters (LLaVA [40], xGen-MM (BLIP-3) [84], and CogVLM [76]). We also test the efficacy of the resulting adversarial image-caption pairs as a poison attack on end-to-end model training. *Next*, we consider and evaluate multiple potential defenses against AMP attacks, and potential attack variants that target such defenses. *Finally*, we consider the efficacy of AMP attacks on closed commercial VLMs, and AMP-enabled poison attacks on models trained on the resulting data.

We summarize our key findings as follows.

- Our analysis of existing model documentation shows that all modern text-to-image models (since the release of DALLE-3) that disclose their image labeling methodology rely on VLMs to label training images.
- Images modified by AMP attacks induce VLMs to produce desired incorrect captions with high precision (90+% CLIP similarity)

and high success rate (70+%) on all tested VLMs. The results are consistent across two large image datasets and a variety of label extraction prompts.

- Adversarially mislabeled image-caption pairs are highly successful at poisoning specific prompts in all tested text-to-image models (SD2.1, SDXL, FLUX) with 94%–99% success rate. Downstream models respond to affected prompts with images that instead match the attacker's target, i.e., a prompt for "cow" produces images of sunflowers. In fact, AMP-induced poison samples are more potent than normal dirty-label poison samples, i.e., benign images paired with incorrect captions.
- Image transformations as a defense can successfully disrupt most AMP perturbations, but AMP attacks can be augmented to make them robust against basic transformations. More powerful defenses such as DiffPure can succeed, but pay a higher price in the form of images that produce lower quality labels.
- Finally, we find that AMP attacks can be augmented to improve transferability to black-box VLMs. Experiments show strong attack success against VLMs on Microsoft Azure and Google Vertex platforms, and that resulting mislabeled image-caption pairs can successfully poison downstream models.

Our work provides a first look at the feasibility of adversarial mislabeling poison attacks against VLM captioners, and suggests that they do pose a threat to generative text-to-image models. While existing defenses can mitigate current attack variants, they require computational and quality tradeoffs that are unattractive at scale. These results further suggest a cat-and-mouse game in defending VLMs against adversarial perturbations, a process that is likely to raise the overall cost of model training on scraped images.

2 Background and Related Work

We begin by providing some background and context on text-to-image diffusion models, vision language models and their use as image caption generators, and related work on adversarial attacks against VLMs and diffusion models.

Text-to-image diffusion models. Diffusion-based text-to-image generation models such as DALLE- 3 [5], Imagen [57], Stable Diffusion 1.5 [70], SDXL [50], and many more [34, 54, 67, 68] have shown remarkable ability to generate high-fidelity synthetic imagery. Diffusion models often undergo multiple rounds of re-training or fine-tuning [22, 48, 58, 69], as demonstrated by Stable Diffusion's SD and SDXL models building on its predecessors. This iterative approach allows for quality improvements and domain specialization in systems [48, 58, 74]. However, repeated re-training also adds security vulnerabilities, as adversaries can inject a small volume of malicious samples to significantly influence subsequent model behavior [77, 91].

Vision-language models. VLMs are vision-integrated language models that jointly encode visual and textual data into a shared embedding space. Trained on large-scale image-caption pairs, VLMs capture relationships between visual and language features, enabling tasks like image captioning.

VLMs as image caption tools. Earlier diffusion models [54, 56, 70] were trained on billions of web-scraped image-caption pairs like LAION-5B [60], which pair images with captions inferred from HTML or alt-text tags. Studies showed that these captions are low quality, and produce training data that leads to degraded model performance [44, 61]. More recent models such as DALLE-3, SANA, FLUX, PixArt [5, 6, 12, 13, 72, 81] use VLMs (e.g., LLaVA, CogVLM, xGen-MM (BLIP-3), MiniGPT-4 [40, 76, 84, 94]) to generate detailed and semantically rich captions from images, producing high quality image-caption pairs for training diffusion models.

Adversarial attacks on VLMs. VLMs are susceptible to adversarial attacks that disrupt the alignment between their visual and text embeddings [7, 25, 28, 29, 52, 64, 87, 92, 93]. Given an image, attackers can compute imperceptible perturbations that manipulate a VLM into producing erroneous captions that do not match image contents [25, 83, 92]. Such attacks can be targeted or untargeted. Targeted attacks [25, 92] perturb an image so that VLMs will produce some predetermined target caption for that image. An untargeted attack [29] simply perturbs images so that a VLM would produce incorrect captions for them.

Adversarial attacks on VLMs can impact a wide range of downstream tasks - from autonomous driving, where perturbed visual inputs can mislead the model's understanding of road signs [14, 46, 90], to VLM-powered multimodal agents, where perturbed images steer the agent towards unintended behavior [79, 82].

Data poisoning attacks on diffusion models. Compared to data poisoning attacks on classifiers [17, 18, 33, 45, 78, 85], attacks on diffusion models are limited. Prior work shows that adversaries can attack diffusion models by injecting triggers through natural language prompts [16, 21, 35, 89] with the assumption that attackers can access the diffusion process or by poisoning the training set [49]. These attacks rely on controlling both the image and the text for given training samples.

More recent work shows that clean-label poison attacks can be successful against large diffusion models [24, 63]. These attacks do not require the attacker to have control over the captions for the poison samples, as long as the captions are clean, making them more stealthy than traditional dirty-label poison attacks. However, they do require white-box access to the diffusion model itself.

In this paper, we explore a new angle in data poisoning by targeting the early stages of the diffusion model training pipeline with adversarial examples generated against VLMs. This method combines the stealthiness of clean-label attacks with the disruptive impact of dirty-label approaches, offering a novel way for compromising diffusion models at their training data preparation phase.

3 Feasibility and Threat Model

The goal of our work is to explore the feasibility and potential impact of poison attacks on text-to-image models, which induce VLMs to produce erroneous labels, effectively making VLMs inject poison image labels into the training pipeline for the attacker. Figure 1 illustrates such an attack. In this section, we first discuss the role of VLMs in producing training data for text-to-image models, and then define the assumptions and threat model for our work.

3.1 SOTA Models Use VLMs to Caption Images

Our first task is to fully understand the role that VLMs play in the training pipeline for today's generative text-to-image models. To

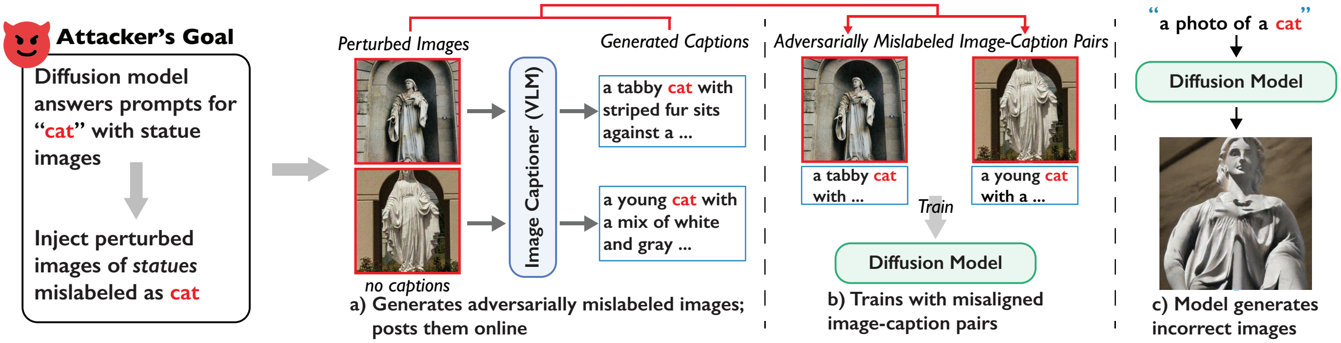
Attacker's Goal
Diffusion model answers prompts for "cat" with statue images
Inject perturbed images of statues mislabeled as cat
Perturbed Images
no captions
Image Captioner (VLM)
Generated Captions
a tabby cat with striped fur sits against a ...
a young cat with a mix of white and gray ...
a) Generates adversarially mislabeled images; posts them online
Adversarially Mislabeled Image-Caption Pairs
a tabby cat with ...
a young cat with a ...
Train
Diffusion Model
b) Trains with misaligned image-caption pairs
"a photo of a cat"
Diffusion Model
c) Model generates incorrect images

Figure 1: An adversarial mislabeling poison (AMP) attack on a diffusion model. An attacker wants to poison a downstream model to produce images of statues when prompted for "cat." They add imperceptible perturbations to benign images of statues (a), so that VLMs will produce captions for them involving cats. A downstream model trained on these image-caption pairs will (b) learn to associate a "cat" with statue characteristics, and (c) produce images of statues when prompted for "cat."

do this, we survey 13 popular text-to-image models to understand captioning procedures used in practice, from the most recent text-to-image models such as SANA [81] back to the first generation of diffusion models like Stable Diffusion SD1.5 [70]. For each model, we identify the following properties based on its corresponding publication or official online documentation.

- **Internet Data:** whether the model was trained at least partly using image data collected from the internet.
- **Synthetic Captions:** whether the model pipeline employs a VLM to generate captions for its image dataset.
- **Public VLM:** whether the VLM used to generate captions is public, e.g., model weights are publicly available.

Our findings are summarized in Table 1. We are unable to obtain any concrete information about training data or source of image captions for 3 of the 13 models (SDXL, Lumina-T2X, and FLUX). Out of the remaining 10 models, 9 explicitly mention the use of images collected from the internet. We note that in 2023, OpenAI's GPT/DALLE-3 technical report was the first to state that training on images captioned by VLMs significantly improved model performance. Since then, all models with documentation on training data explicitly mention using VLMs for captioning. With the exception of OpenAI and Google, who used in-house VLMs, all other models post 2023 used a publicly available VLM.

Models	Creator	Released Date	Training Pipeline Properties		
			Internet Data	Synthetic Captions	Use Public VLM
SD1.5 [70]	Stability	10/2022	✔	✗	✗
SD2.1 [71]	Stability	12/2022	✔	✗	✗
GPT/DALLE-3 [5]	OpenAI	8/2023	✔	✔	✗
PixArt-α [12]	Huawei	9/2023	✔	✔	✔
Kolors [72]	Kuaishou	2/2024	✔	✔	✔
PixArt-Σ [13]	Huawei	3/2024	✔	✔	✔
Hunyuan-DiT [39]	Tencent	5/2024	✔	✔	✔
SD3 [27]	Stability	6/2024	✔	✔	✔
Gemini/Imagen 3 [23]	Google	8/2024	✔	✔	✗
SANA [81]	Nvidia	10/2024	—	✔	✔
SDXL [50]	Stability	6/2023	—	—	—
Lumina-T2X[30]	ShanghaiAI	6/2024	—	—	—
FLUX [6]	Black Forest	8/2024	—	—	—

Table 1: Aside from models with no documentation on training data and captions (SDXL, Lumina, FLUX), all models since GPT/DALLE-3 have adopted VLMs for caption generation.

3.2 Threat Model

We now describe our threat model, including our assumptions on the model training process and capabilities of the attacker. First, we assume that the model trainer is training on images downloaded from the Internet, and uses a VLM to generate accompanying captions. Based on our results above, both are common practices. We consider two scenarios, where a model is trained using a prior model as base, and where a model is trained from scratch.

The attacker. The attacker's goal is to manipulate the behavior of a text-to-image model so that it produces images inconsistent with the prompt it receives. We make minimal assumptions about the attacker's capabilities, including:

- They have access to moderate consumer-grade GPUs.
- They are able to inject a small number of images into the model's dataset of downloaded images. This has already been demonstrated in the wild by prior researchers [8].
- They have white-box access to the VLM used in the training pipeline. We relax this assumption later (see below).

Black-box threat model. While most companies/model trainers use open source VLMs, some AI companies build customized VLMs that are not fully available to attackers in a white-box setting. To address this scenario, we relax the assumption of white-box access to VLMs, and consider these attacks under this new threat model later in the paper (§8).

4 Adversarial Mislabeling Poisoning

In this section, we introduce the concept of *Adversarial Mislabeling Poison* (AMP) attacks, poisoning attacks that manipulate VLMs in order to inject poison samples into the model training pipeline. We also give details of a sample implementation, and describe how it is able to poison specific prompts in a text-to-image diffusion model by attacking the VLM that labels training images.

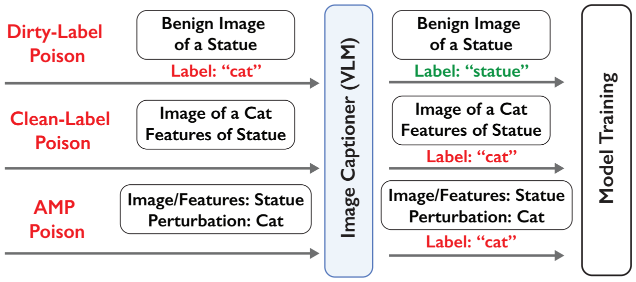

Figure 2: Different poison attacks on a training pipeline with a VLM image captioner. The label of a dirty-label poison is "corrected" by the VLM. A clean-label poison image gets the correct label but teaches the downstream model wrong visual features. An AMP poison image tricks the VLM into giving it the wrong caption, thereby creating a poison sample similar to a dirty-label sample.

4.1 VLMs and Poison Attacks

Before introducing AMP, we first consider how existing poison attacks work on modern diffusion models. Traditionally, poison attacks on machine learning models try to associate an incorrect label with a particular set of visual features, e.g., the label "cat" with visual features of a statue. These attacks are often grouped into two categories, dirty-label and clean-label attacks. Dirty-label attacks simply pair a benign image (statue) with the incorrect label ("cat"). In contrast, clean-label attacks can pair the label "cat" with an image of a cat, but modify the image to contain hidden features of a statue.

Both dirty and clean-label poison attacks face challenges in modern training pipelines that use VLMs to caption images. Figure 2 illustrates how these attacks interact with a VLM. First, dirty-label poison samples rely on an image associated with a mismatched caption. These attacks fail because the VLM will generate the correct caption and overwrite any mismatched captions. Next, clean-label poison samples are not affected by VLMs, since their visual feature shift do not transfer to VLMs. Recent work on Nightshade [63] is an example of such attack against diffusion models and explicitly demonstrated the immunity to VLM captioners. However, these clean-label attacks are limited by the fact that, to compute an effective feature perturbation, they require knowledge of the feature space of the model being trained. Clean-label poisons computed for one model are likely to have low impact on other models.

VLMs as stepping stones in a poison attack. Adversarial Mislabeling Poisons (AMPs) are different from both dirty-label and clean-label poisons. An adversarially mislabeled poison sample is a benign image altered specifically with the goal of ***fooling a VLM into producing the wrong image caption.*** The goal is not to pass by the VLM unnoticed, but to manipulate the VLM into producing the mismatching caption itself. For the example shown in Figure 2, an AMP image with benign features of a statue induces a VLM into labeling it as a "cat," thereby achieving the same effect as a dirty-label poison attack.

Using the VLM to produce poison samples presents multiple advantages for an attacker. First, as we showed in §3.1, VLMs are ubiquitous today in model training, and attacks targeting a single VLM can potentially affect multiple downstream models which use this VLM to caption images. Second, VLMs are generally integrated into model training pipelines to enable fast processing of millions of images. It would be logistically challenging (and impractical) to verify the results of VLMs, especially given the large volume (e.g., millions) of training samples.

Poisoning individual prompts via adversarial mislabeling. Existing work has shown that individual prompts or "concepts" in text-to-image models can be manipulated by adversarial poison samples [63]. The key observation is that the volume of benign training samples for any single concept might be small enough for an attacker to overcome. For example, an attacker can corrupt a model to always produce statue images when prompted for "cat."

In our work, we are interested in whether adversarial mislabeling poison attacks can produce similar effects on diffusion models. To be more precise, the attacker's objective is to make a model respond incorrectly to a *target concept* and output images associated with a *reference concept*. Applied to our cat and statue example above, "cat" is the target concept for the poison attack, and "statue" is the reference concept a compromised model will output in response – the model outputs statue images when prompted for "cat."

4.2 Implementation of an AMP Attack

We now discuss detailed decisions towards a full implementation of an AMP attack.

Perturbation methods against VLMs. Recent work has seen a number of different approaches to perturbing images that lead to incorrect VLM behavior [7, 25, 28, 29, 52, 64, 87, 92, 93]. From these options, we choose a method for generating VLM mislabels that best aligns with the requirements of AMP poison attacks.

Our attack implementation uses the *image-to-image* adversarial perturbation algorithm from [92]. This algorithm starts from a clean image, and iteratively computes pixel perturbations on this image to minimize the distance between the perturbed image and a target image in the VLM feature space, subjecting to a perturbation budget. Compared to image-to-text and diffusion-based non-L_p attacks [79, 92], this attack method achieves a stronger mislabeling effect against VLMs. Furthermore, this method also prompts VLMs to generate highly detailed captions, effectively bypassing filters designed to eliminate low-quality or vague descriptions.

Perturbation algorithm for adversarial mislabeling. We assume the attacker has an image collection grouped by the concept, e.g., images of cats, statues, drones, etc.

Given a target/reference concept pair, we first select a clean image x_t from the target concept group, and a clean image x_r from the reference concept group. The goal is to perturb the reference image x_r so that the perturbed image $x_r + \delta$ will be mislabeled by the VLM to "mimic" the caption of x_t. This is defined by:

$$\min_{\delta} \text{Dist}(\phi(x_r + \delta), \phi(x_t)) \quad \text{subject to } |\delta| < \epsilon \tag{1}$$

where ϕ denotes the VLM's image feature extractor, Dist(.) measures the feature space distance.

Figure 3 shows two examples of adversarially mislabeled image-caption pairs produced by our AMP implementation (discussed next), where the target/reference concept pairs are cat/statue and firework/drone, respectively. CogVLM is used to caption images.

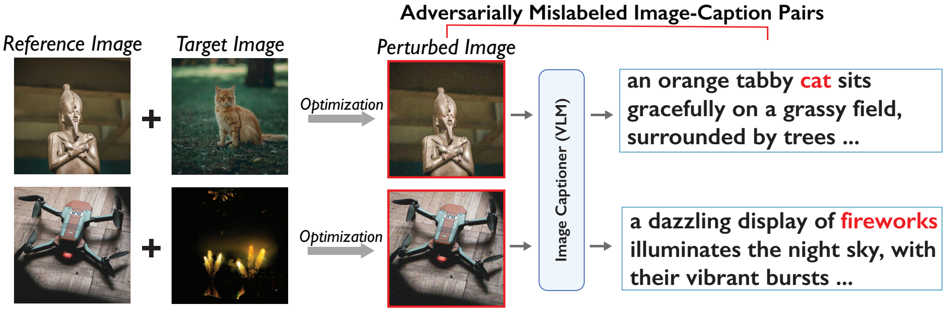

an orange tabby cat sits gracefully on a grassy field, surrounded by trees ...

a dazzling display of fireworks illuminates the night sky, with their vibrant bursts ...

Figure 3: Based on two (clean) target and reference images, AMP produces an adversarial image (marked by a red box), which are wrongly captioned by the VLM, producing adversarially mislabeled image-caption pair. CogVLM is used as the captioner.

Grouping images by concepts. The above algorithm needs to group images by concept, i.e., associate each image with a single concept. Rather than manually inspecting images, we propose to automate the process as follows: for each image, use its caption (original or via a captioner) to extract a set of candidate concepts as the main objects/actions; feed the image and each candidate concept (y) into a CLIP model to obtain y's confidence score; select the candidate concept with the highest confidence as the concept label of the image, and save its confidence level. As such, each image is now associated with a single concept and its confidence score.

5 Experimental Evaluation

In this section, we experimentally study the efficacy of our AMP prototype, using popular open-source VLMs and text-to-image diffusion models. We aim to evaluate the two distinct stages of the attack: (1) producing adversarially perturbed images to be mislabeled by the VLM-based image captioner, and (2) poisoning text-to-image models using these mislabeled image-caption pairs, targeting specific prompts. This allows us to conduct an in-depth analysis on the "core leverage" of AMP and its end-to-end effectiveness.

In the following, we first describe the experimental setup, including the image datasets, the VLMs and diffusion models, and the parameters used for adversarial perturbation and poisoning experiments. This is followed by two sets of metrics to evaluate the mislabeling and end-to-end poisoning performance. Next, we present the key results on the two attack stages.

5.1 Experimental Setup

Datasets. We use two, large-scale image datasets: LAION Aesthetics (LA) [59] and Photo-Concept-Bucket (PCB) [51]. Both contain over 500,000 high-quality images. All images are resized to a resolution of 1024x1024.

VLMs. We consider three popular open-source VLMs: LLaVA [40], xGen-MM (BLIP-3) [84], and CogVLM [76]. All three have been adopted by model practitioners for generating image captions to train text-to-image diffusion models [12, 27, 37, 42, 62]. Each VLM uses a distinct ViT image feature extractor, along with varying language model components. While these VLMs share a similar high-level architecture, they are each notable for the following novel characteristics. The earliest model, LLaVA, showcases the power of a fully-connected layer between text and vision. xGen-MM (BLIP-3) is one of the first to introduce training via single unified objective. CogVLM replaces commonly used "shadow" alignment between text and vision features by training a separate expert module to increase richness in image-caption alignment.

When operating each VLM as an image captioner, by default, we use the prompt: "Describe the image in twenty words or less." This is also the default prompt provided by the most popular GitHub VLM repository [36].

Text-to-image diffusion models. We consider four different, open-source diffusion models: SD1.5 [70], SD2.1 [71], SDXL [50], and FLUX [6]. Each has gained significant popularity at various points over the past few years. They differ primarily in architecture (e.g., model components and size) and training process/data. The first three SD models use the initially popular UNET model to perform denoising, while FLUX employs the increasingly favored DiT architecture. Additional details on architectural differences and pretraining parameters are listed in Appendix A.1.

Selecting target and reference concepts. We use the grouping method presented in §4.2 to categorize images by concepts. We use the original captions provided by PCB and LLaVA to generate captions for LA images. We then identify, for each of the two datasets, the top 100 concepts (i.e., those with the most images) and randomly select target and reference concepts from these groups.

Adversarial perturbation. We generate adversarially perturbed images using the perturbation algorithm defined by Eq. (1) (§4.2). The default perturbation budget (L_∞ or maximum per-pixel change) is set to $\frac{16}{255}$. Given a target/reference concept pair, we select the corresponding target and reference images that are strongly aligned with their associated concept (confidence score > 0.99).

Training diffusion models. We consider two training scenarios: training a model from scratch and fine-tuning a pretrained model. Since training diffusion models from scratch is computationally challenging (>10 days on a single A100 GPU for the smallest model SD1.5), we consider the following setup:

- SD1.5: training from scratch, using a training dataset consisting of $\sim$500,000 image-caption pairs. With the goal of poisoning 25 target concepts, by default, this training data contains 500×25 adversarially mislabeled poison samples.

- SD2.1, SDXL and FLUX: fine-tuning a pretrained model, using 12,500 image-caption pairs. To poison 25 concepts, this dataset contains 125×25 adversarially mislabeled poison samples.

We provide the detailed training setup (sources of training scripts and parameters) in Appendix A.1.

5.2 Evaluation Metrics

For a comprehensive evaluation of the AMP attack, we introduce two sets of metrics targeting distinct stages of the attack process: (1) the effectiveness of generating adversarial images that are mislabeled by the VLM-based image captioner, and (2) the effectiveness of the resulting adversarial image-caption pairs as poison attack on the text-to-image diffusion model.

Evaluating effectiveness of mislabeling. We introduce three metrics to evaluate the attack success rate and the level of control in achieving the mislabeling effect.

- **Mislabel success rate (MSR)** – This metric measures the probability of a perturbed image being successfully mislabeled by the VLM captioner. Given a target and reference concept pair, the perturbed image is considered **successfully mislabeled** if the caption generated by the VLM satisfies all three of the following conditions: (1) the caption does not contain the reference concept, (2) the caption does contain the target concept, and (3) the CLIP similarity between the caption and the target image is greater than the CLIP similarity between the caption and the reference image. The first two conditions use exact string matching [1] to ensure that the caption of the perturbed image describes the target concept and excludes the reference concept. The third condition accounts for cases where the caption contains terms that are semantically related to either concept (e.g., "puppy" instead of "dog"), ensuring that the caption is more semantically aligned with the target image than with the reference image. We discuss the detailed implementation of the third condition in Appendix A.2.
- **Adversarial alignment rate (AAR)** – This evaluates how tightly the adversarially perturbed image aligns with its intended target. Let x_i be a clean, unperturbed image, and $x_i + \delta_i$ be its adversarially perturbed version. Let $x_{i,t}$ be the target image used to perturb x_i. Among N test images, we compute:

$$\text{AAR} = \frac{1}{N}\sum_{i=1}^{N}\frac{sim(x_{i,t}, vlm(x_i + \delta_i))}{sim(x_{i,t}, vlm(x_{i,t}))}$$

  where $vlm(x)$ is the caption of x produced by the VLM, and $sim(.)$ measures the CLIP similarity between a caption and an image. Intuitively, AAR is within [0,1] and a strong targeted AMP attack will lead to a high AAR value (i.e., AAR→ 1).
- **Benign alignment rate (BAR)** – To evaluate the alignment between the adversarially perturbed image and its original state (without perturbation), we compute the following:

$$\text{BAR} = \frac{1}{N}\sum_{i=1}^{N}\frac{sim(x_i, vlm(x_i + \delta_i))}{sim(x_i, vlm(x_i))}$$

  Again, BAR is within [0,1]. And a strong AMP attack should have a very low BAR value (i.e., BAR→ 0).

Dataset	VLM	MSR (↑)	AAR (↑)	BAR (↓)
LA	LLaVA	0.73	0.90	0.05
	BLIP-3	0.71	0.94	0.04
	CogVLM	0.72	0.93	0.06
PCB	LLaVA	0.89	0.94	0.04
	BLIP-3	0.93	0.97	0.04
	CogVLM	0.91	0.96	0.04

Table 2: Adversarial images achieve high mislabeling success (MSR) across datasets and VLM architectures without revealing original concepts.

Prompt	AAR (↑)	BAR (↓)
Describe the image in twenty words or less.	0.96	0.04
Caption this image accurately, with as few words as possible.	0.98	0.04
Provide the most detailed caption.	0.95	0.04
Caption this image accurately, without speculation. Just describe what you see.	0.95	0.04
What's in this image?	0.94	0.04

Table 3: Adversarial images remain effectively mislabeled, even when prompting CogVLM with different prompts.

Evaluating effectiveness of poisoning text-to-image models. Assuming the adversarial image-caption pairs are designed to poison a specific concept C in the text-to-image diffusion model, we evaluate the poison effectiveness by examining the images generated by prompting the model with C[2].

- **Poison success rate (PSR)** measures the probability that when prompting the model with C, the generated image does not reflect the concept C. Following prior work on poison attacks [63], we use a zero-shot CLIP model [53] to classify each image into one of the top 100 concepts of the current image dataset (LA or PCB). Note that C is among the top 100 concepts.

  PSR (C) = 1 − % of generated images being classified as C

  Our calculation uses 10 generated images per target concept C. We report the average PSR across 25 C choices. As reference, for a clean SD2.1 model, PSR ∼0.09.

5.3 Adversarial Mislabeling is Effective

Our experiments start by looking at the first stage of the AMP attack: efficacy of adversarial mislabeling on different VLMs. For each image dataset (LA and PCB), we pick 25 pairs of target and reference concepts from the top 100 most frequently used concepts, and report averaged results from mislabeling attempts. Table 2 summarizes the attack outcomes in terms of MSR, AAR, and BAR

[1] We lemmatize the nouns in each caption prior to matching.

[2] We use text prompts from a held out validation set of our image datasets, where C defines the object/action.

for the two image datasets (LA and PCB) on each of the three VLMs (LLaVA, BLIP-3, and CogVLM).

The results are shown in Table 2, and are highly consistent. Across the three VLMs, the average mislabeling success rate (MSR) is high, 0.72 for LA and 0.91 for PCB. Of the successfully mislabeled adversarial images, there is little discrepancy across VLMs in adversarial or benign alignment ratio (AAR, BAR), though it tends to be slightly more successful against PCB (AAR = 0.96) than LA (AAR = 0.92). This trend in both MSR and adversarial alignment may be attributed to the higher detail in PCB images, many of which are high-resolution photographs, compared to images in LA, which often contain single objects set in the foreground with a primarily empty/white background. This decrease in image detail likely leaves less room for the optimization algorithm to hide perturbations useful for mislabeling.

Varying VLM prompts. We now explore the impact of mislabeling when different prompts and requested level of detail are used to extract a caption from the VLM. Based on popular GitHub diffusion model training and captioning repositories [3, 36], we identify four additional prompts covering different levels of caption detail. These prompts are listed in Table 3 along with AAR and BAR results. In general, we see negligible impact on adversarial images from the use of different image captioning prompts. Results for CogVLM are representative of other VLMs.

Varying image perturbation budget. Next, we explore how different perturbation budgets used during image optimization affect mislabeling efficacy. Following prior literature on adversarial examples, we test with the following maximum per-pixel changes: $\frac{2}{255}, \frac{4}{255}, \frac{8}{255}, \frac{16}{255}, \frac{32}{255}$, and attempt to generate 8 mislabeled images for each of the 25 reference/target pairs in the PCB dataset against CogVLM, the highest performing captioner. In Figure 4, we show that increasing the budget naturally increases the mislabel success rate, though not significantly after $\frac{16}{255}$. In Figure 5, we show that low perturbation budgets can still lead to effectively mislabeled adversarial images. However, there is a tradeoff in AAR (0.6 at $\epsilon = \frac{2}{255}$ compared to 0.96 at $\epsilon = \frac{16}{255}$). Interestingly, we also find that perturbation budget has a negligible impact on the length of captions generated by adversarially mislabeled images. In Figure 6, adversarially mislabeled images of all perturbation budgets share a very similar distribution of caption length to benign images, with an average character count ~120.

5.4 Adversarially Mislabeled Images Successfully Poison Diffusion Models

Earlier results confirmed that adversarial mislabeling attacks are effective at inducing targeted captions by VLMs. The next step is to evaluate if the resulting image-caption pairs are effective as poison training samples against diffusion models.

Poisoning is effective across datasets & VLM captioners. In this experiment, we fine-tune SD2.1 models using a total of 12,500 image-caption pairs. With the goal of poisoning 25 concepts, this dataset contains 125×25 adversarially mislabeled poison samples (i.e., 125 poison samples per target/reference concept pair). In this experiment, every poison sample is successfully mislabeled. In practice, the attacker does not know how many of their injected poison samples are successfully mislabeled by the captioning system. Thus, their most effective strategy is to inject as many poison samples as possible. Our experiment simulates the outcome of such attack effort as 125 samples per concept pair being successfully mislabeled, and examines their impact on the subsequent model training.

In Table 4, we report the poison success rate (PSR) for two datasets (LA, PCB) and three VLMs. We see that poisoning diffusion models with adversarially mislabeled images is effective, where the average PSR is ~0.90.

Poison is effective across model architectures. We repeat the experiment on two larger diffusion models, SDXL and FLUX, using the highest quality dataset and VLM captioning pair (PCB and CogVLM), and show the results in Table 5. Compared to a PSR of 0.95 for SD2.1, the same adversarially mislabeled images are just as or even more successful at poisoning SDXL (0.94 PSR) and FLUX (0.99 PSR). It is interesting to note that adversarially mislabeled images poisoned the DiT model (FLUX) slightly more effectively than the two UNET-based models (SDXL, SD2.1). Since adversarially mislabeled images introduce misaligned image-caption pairs into the dataset, it should intuitively transfer without modification to different diffusion model architectures. Examples of corrupted images generated by SDXL can be found in Figure 8, which clearly show that the fine-tuned SDXL model no longer generates images accurately. In fact, we observe that generated images often directly match the destination concept (ideal outcome for the poison attack).

Adversarially mislabeled images outperform dirty-label. At a high level, AMP should impact trained models in the same way as traditional dirty-label images, where benign images have their captions manually altered. In Table 5, we also compare the poison efficacy of adversarially mislabeled images to that of dirty-label images (unperturbed images with manually changed captions). For consistency, the dirty-label images use the same target/reference concept images used to generate the AMP images.

Surprisingly, we find that the AMP poison success rate is generally higher than that of the dirty-label variant (Tables 4, 5). We hypothesize that adversarially mislabeled images are more potent because they are perturbed, which results in more significant backpropagation updates and forces diffusion models to "change more" in the same number of steps than normal unperturbed images. This is verified in our observation in Figure 7, which shows that adversarially mislabeled images introduce higher loss when evaluated against SD2.1 than dirty-label image-caption pairs.

Poison is effective even at low doses. While poisoning is effective, we expect the potency of the poisoning attack to scale with the number of AMP images injected into the training set. We confirm this in Table 6 by fine-tuning multiple SD2.1 models each with different amounts of poison images. We find that the sharpest change in poison success rate occurs between 0 and 25 adversarially mislabeled images. 25 images is already sufficient to produce a poison success rate of > 0.6. This suggests that even if attackers are able to inject only a small volume of adversarially mislabeled images into training datasets, they will still have a non-trivial impact on the quality of images generated for targeted concepts.

Training from scratch. Due to the computational cost of training diffusion models from scratch (10 days on a single A100 GPU

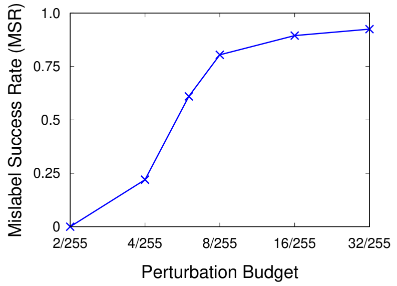

Figure 4: Adversarial images are successfully generated after $\epsilon = \frac{4}{255}$, reaching 91% MSR at $\epsilon = \frac{16}{255}$.

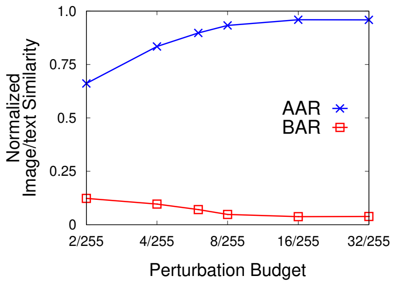

Figure 5: Mislabeled images do not leak benign captions (low BAR) even at the lowest budget, while still effectively mislabeled (high AAR).

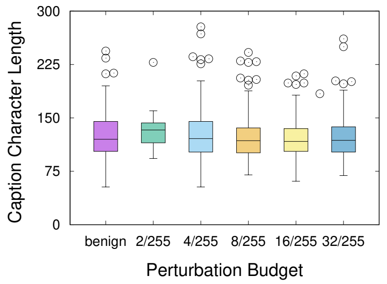

Figure 6: Adversarially mislabeled images generate captions of similar length to benign images.

Dataset	VLM	Adversarially Mislabeled	Dirty-Label
LA	LLaVA	**0.92 ± 0.02**	0.88 ± 0.02
	BLIP-3	**0.92 ± 0.02**	0.83 ± 0.02
	CogVLM	**0.88 ± 0.02**	0.87 ± 0.02
PCB	LLaVA	**0.90 ± 0.02**	0.86 ± 0.02
	BLIP-3	**0.98 ± 0.01**	0.92 ± 0.02
	CogVLM	**0.95 ± 0.01**	0.85 ± 0.02

Table 4: Poison success rate when SD2.1 models are trained on adversarially mislabeled image-caption pairs. Notably, poisoning using adversarially mislabeled images is equivalent or stronger than using dirty-label images. Poison success rates (PSR) are shown alongside ± standard deviation.

Model	Adversarially Mislabeled	Dirty-Label
SD2.1	**0.95**	0.85
SDXL	**0.94**	0.93
FLUX	0.99	**1.00**

Table 5: Poison effects across architectures (in terms of PSR). AMP images generated against CogVLM on the PCB dataset are highly successful at poisoning two large diffusion model architectures: SDXL and FLUX.

for one model), we only trained a single SD1.5 model on the largest dataset (LAION-Aesthetic) using the fastest VLM, LLaVA. Training details are in Appendix A.1. When we poison the dataset to include 500 adversarially mislabeled images for each target/reference concept pair, we found a PSR of 0.97 for the SD1.5 model. This confirms that adversarially mislabeled poison images can successfully poison models in both training-from-scratch and continuous model training scenarios.

6 Countermeasures

Having established the efficacy of AMP attacks, we now turn our attention to potential countermeasures. Once again, we focus on the two distinct stages of the attack: first, applying the use of image transformations to prevent mislabeling by VLMs, then, filtering training data to remove poison image-caption pairs.

# of Poison Samples	0	25	50	75	100	125
PSR	0.09	0.58	0.82	0.87	0.89	0.95

Table 6: Poison success increases as number of adversarially mislabeled poison samples increases. Results shown represent average PSR across all concepts tested. The sharpest jump occurs between 0 and 25, suggesting even a small amount of mislabeled images can effectively poison single concepts in large models.

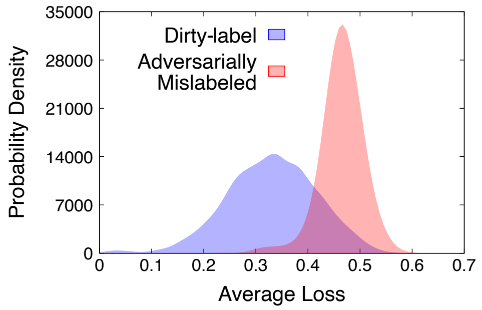

Figure 7: Adversarially mislabeled image-caption pairs have higher loss on pretrained SD2.1 model than dirty-label.

The results reported in this section are from experiments using CogVLM (the best performing VLM), the PCB dataset, the top 4 most potent target-reference concept pairs (i.e., those with the highest MSR in the absence of countermeasures), and the SD2.1 model (fine-tuning-based model training).

6.1 Image Transformations

Image transformations are a widely used technique for defending against adversarial perturbations [4, 26, 32]. In our problem setting, the model trainer applies image transformations to the entire image set before passing them to the VLM captioner. The generated captions are then paired with the original, untransformed images and passed to the subsequent model training pipeline.

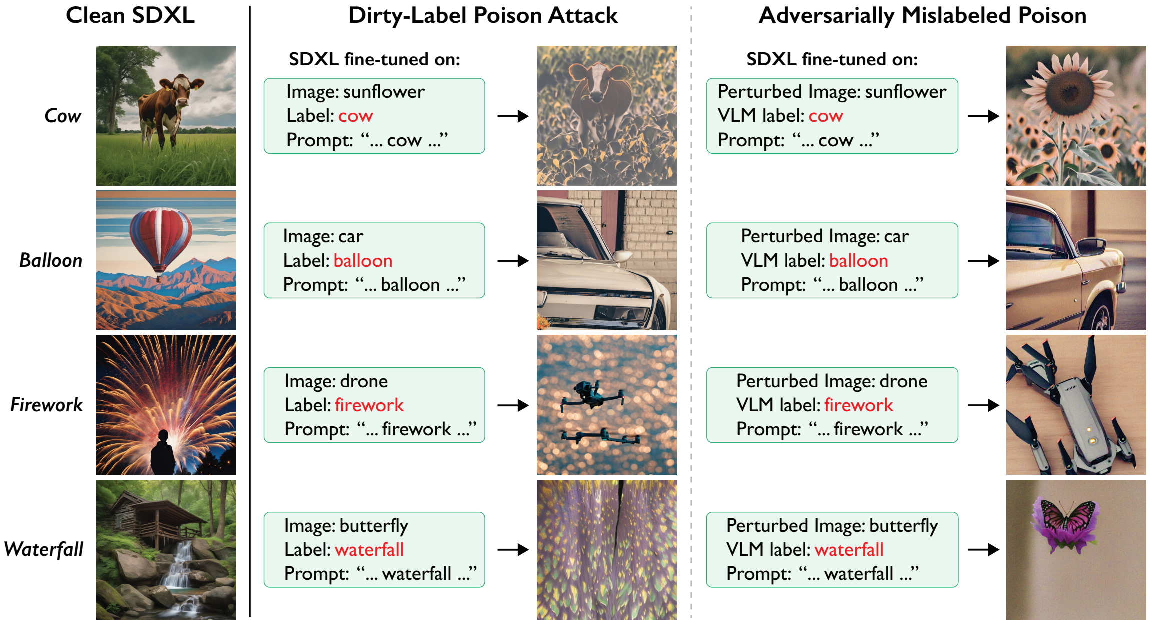

Figure 8: Examples of images generated by SDXL models after being trained on dirty-label images and adversarially mislabeled images. The original clean SDXL is included for comparison.

Image Transformation	MSR		PSR	
	Basic Attack	Adaptive Attack	Basic Attack	Adaptive Attack
JPEG Compression	0.00	**0.89**	0.04	**0.94**
Gaussian Blur	0.11	**0.42**	0.09	**0.76**
Gaussian Noise	0.26	**0.63**	0.58	**0.86**

Table 7: Applying transformations on images before passing them into VLM effectively reduces both mislabeling success rate (MSR) and poison success rate (PSR) of the basic attack (§4.2). An adaptive attack can bypass these defenses (§7.1).

We experimented with three transformation methods: JPEG compression, Gaussian blur, and Gaussian noise, with the goal of reducing image noise. Table 7 shows that image transformation can effectively reduce both mislabeling success rate (MSR) and poison success rate (PSR) of the basic attack. JPEG compression is the most effective and completely eliminates the mislabeling effect. This aligns with prior findings [4, 26, 32].

Although image transformations may seem highly effective at preventing mislabeling, they can be bypassed by adaptive attacks that account for their effect during perturbation optimization, as we will show in §7.1.

6.2 Filtering Training Data

Before submitting the image-caption pairs into the training pipeline, the model trainer can perform a final-stage check to filter out potential poison/adversarial samples. We consider four potential filtering metrics with increasing computational complexity. We evaluate each filtering method by measuring the filtering rate, i.e., the percentage of poison data eliminated, at a fixed false positive rate (FPR) of 0.05. Table 8 lists the filtering rate result for all four methods, which we elaborate below.

Filtering Method	Filtering Rate	FPR
Image Quality	0.06	0.05
Caption Quality	0.01	0.05
Model Loss	0.45	0.05
Image-caption Alignment	**1.00**	0.05

Table 8: Filtering poison training data using four different metrics, at a false positive rate (FPR) of 0.05. The metric of image-caption alignment is the most effective. However, an adaptive attack can bypass these defenses (see §7.1).

Filtering out low-quality images. Adversarial perturbations often correlate with low-quality images, prompting model trainers to use zero-shot quality models like CLIP Aesthetics [75] to filter them out. Unfortunately, it is ineffective against AMP, removing only 6% of poison data at a 5% FPR. As such, ~117 (out of 125) poison samples per target concept are injected into the training pipeline, leading to effective poisoning (shown in Table 6). Finally, Figure 11 (in Appendix) plots the distribution of CLIP Aesthetic scores for benign images and adversarial images at varying perturbation budgets. Even for AMP images using very high perturbation budgets of $\epsilon = \frac{32}{255}$, which is double our current setting, filtering remains ineffective.

Filtering out low-quality captions. Another approach to filtering would be to look at each caption's semantic quality. Following prior work [95], we filter VLM-generated captions by their BLEU scores against a known, high-quality caption distribution. As expected, AMP's adversarial images, while causing mislabels, do not degrade the caption quality. Thus, this filtering method is also ineffective, removing 1% of mislabeled images at a 5% FPR.

Filtering out high-loss image-caption pairs. Earlier, Figure 7 shows that AMP's image-caption pairs lead to higher loss in the diffusion model. This pattern can be leveraged to filter out poison samples. Our experiments show that it removes 45% of the AMP poison samples. Given the demonstrated potency of these poison samples, this level of filtering is insufficient to protect downstream diffusion models (see Table 6). Finally, the benign training samples also removed by this filter are likely biased toward new data that is crucial for improving the model, especially when training on fresh/edge cases [66].

Filtering misaligned image-captions. This is the key property that defines AMP's mislabeled image-caption pairs. One can compute the alignment score (i.e., CLIP similarity) between each image and its caption, and remove those with low alignment scores. This filtering method turns out to be the most effective, removing all poison samples at 5% FPR.

7 Bypassing Countermeasures

Defenses against adversarial perturbations are known to be susceptible to adaptive attacks [2, 9, 73, 86]. In this section, we explore how an attacker can leverage adaptive techniques to bypass countermeasures. We adopt the same threat model as prior research on adversarial machine learning [73, 80, 88], assuming the attacker has white-box access to the defenses implemented by the model trainer, including their methodologies and parameters.

In the following, we first present the adaptive attack design, aimed at overcoming the countermeasures discussed in §6, and evaluate its effectiveness. Next, we discuss two high-cost defenses that a determined and resourceful model trainer could employ, along with the implications for AMP attacks.

7.1 Adaptive Attack Design

We present an adaptive attack designed to circumvent the two most effective countermeasures in §6, JPEG compression and image-caption alignment-based filtering. We achieve this by adding two additional loss terms to the optimization function for adversarial perturbation.

Regarding JPEG compression, prior work has demonstrated that optimizing perturbation with a differentiable approximation of the JPEG compression on images can produce adversarial images resistant to this transformation [55, 65]. We adopt this strategy and add an additional loss term using the differentiable JPEG approximation provided in [55].

To resist data filtering based on image-caption alignment, we must increase the CLIP similarity score between the adversarial image and its caption, making it comparable to the similarity observed in benign image-caption pairs. We achieve this by incorporating another loss term into the perturbation optimization, ensuring a high CLIP similarity between the perturbed image and the caption of the target image (C_t).

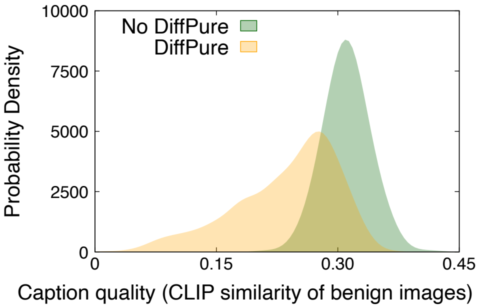

Figure 9: The caption quality of benign images decreases substantially when DiffPure is applied. DiffPure decreases the mean CLIP score of the captions with respect to the original image from 0.31 to 0.24.

The perturbation optimization for the adaptive attack is:

$$\min_{\delta} \quad \text{Dist}(\phi(JPEG(x_r+\delta)), \phi(x_t)) - \alpha \cdot sim(x_r+\delta, C_t) \qquad (2)$$
$$\text{subject to } |\delta| < \epsilon.$$

$JPEG$ is the differentiable function [55] that approximates JPEG compression. $sim(.)$ calculates the CLIP similarity score for the given image and caption.

7.2 Adaptive Attack Performance

We evaluate our adaptive attack against the countermeasures from §6, under the same experiment setup.

Bypassing image transformations. Table 7 shows that the adaptive attack effectively circumvents JPEG compression, increasing the mislabeling rate from 0% to 89%. Interestingly, the adaptive attack also performs well against other transformations (Gaussian noise and blur) despite explicitly optimizing for them. This is likely due to the inherent similarities between various image transformation techniques.

The same table also lists the end-to-end poison result of the adaptive attack against the three image transformation methods. The adaptive attack's PSR is nearly the same as the basic attack in absence of any countermeasure.

Bypassing training data filtering. We evaluate the poisoned image-caption pairs produced by the adaptive attack against the image-caption alignment-based filtering. Recall that previously this measure could remove 100% of the AMP poison samples. The adaptive attack reduces the filtering rate to only 6%, rendering this countermeasure ineffective.

7.3 Determined Model Trainer

Next, we examine the extreme case where a model trainer is determined to eliminate the effect of poisoning, even at the cost of sacrificing performance and allocating significant computational resources. We explore two potential approaches and discuss their implications for AMP attacks.

Diffusion-based image purification. Diffusion-based purification (DiffPure) is an effective yet high-cost image purification technique designed to remove adversarial noise in classifier settings [47]. We apply DiffPure to purify adversarial images generated by AMP, using the code and default setup from the original paper. We use the largest pretrained model provided by the authors, specifically the one for ImageNet, and adhere strictly to the configuration file provided for this model, without deviation.

We run DiffPure on the entire fine-tuning training set, including both benign images and adversarial images generated by the adaptive attack. On these adversarial images, DiffPure reduces the mislabeling success rate (MSR) to 1.7%.

However, we found that DiffPure significantly degrades the image quality and thus the caption quality when the purified image is fed into VLMs. To illustrate this, Figure 9 shows the distribution of CLIP similarity[3] with and without applying DiffPure. We see that DiffPure decreases the average CLIP similarity from 0.31 to 0.24. This results in over 25% of the training dataset being discarded during model training, as model trainers typically remove low-quality text-image pairs with a CLIP similarity below 0.2 [10, 60]. We verify this by training a diffusion model using DiffPured images and their VLM-generated captions, and observe substantial quality degradation when compared to a normal model (details in Appendix A.3).

Finally, we note that running DiffPure is computationally intensive. A small, 50,000 image dataset on a single NVIDIA TITAN RTX GPU takes over 26 days to purify.

Employing multiple VLMs. Rather than use just a single VLM to generate image captions, a determined model trainer could use multiple VLMs for each image, and choose the best option. In fact, this is the approach that Nvidia uses with their SANA model, a recent SOTA text-to-image diffusion model [81]. There, multiple VLMs generate different candidate captions, from which one is randomly sampled using CLIP similarity as the temperature (τ) weighted probability for each candidate ($0 \leq \tau \leq 1$). We mimic this setup using all three VLMs ($n = 3$) and report the results in Table 9 with two edge τ values. Before testing our attack, we first confirm that, under this more complicated captioning system, the diffusion model training remains stable. Specifically, when fine-tuned on benign images captioned by this system, the SD2.1 model leads to a low poison success rate (PSR) of 0.1, comparable to that of a clean SD2.1 model (0.09).

With high selection randomness (maximum temperature $\tau = 1$), this method reduces mislabeling success rate (MSR) to 0.38, although the poison effect is still strong (PSR=0.6). With low selection randomness ($\tau = 0$), our adaptive attack can effectively lead to mislabels (MSR=0.99) by boosting the CLIP similarity between the perturbed image and the target caption. Here we notice that the corresponding PSR is 0.84, which is lower than previous results. This is likely due to the use of "selective" VLMs, which increases the quality (i.e., CLIP similarity) of benign image-caption pairs.

8 Black-box Mislabeling Attack

In this section, we investigate the effectiveness of adversarial mislabeling under a black-box threat model, where the attacker has **no access** to the parameters or architectures of the target VLMs. First, we observe limited transferability of our standard attack (§5) against black-box VLMs (< 1% MSR). Then, we propose a strong attack variant where we enhance the attack's transferability. We show the augmented attack has high transferability to local black-box models (avg. 58% MSR), and even transfers well to commercial VLM models from Google and Microsoft.

VLM methods	**MSR**	**PSR**
Multiple VLMs ($n = 3$, $\tau = 0$)	0.99	0.84
Multiple VLMs ($n = 3$, $\tau = 1$)	0.38	0.60

Table 9: Adaptive attack's performance when multiple VLMs are used to caption images. n is the number of VLMs used; $\tau \in [0, 1]$ is the selection randomness (temperature).

VLM	**MSR (↑)**	**AAR (↑)**	**BAR (↓)**
LLaVA	0.73	0.73	0.05
BLIP-3	0.81	0.75	0.05
CogVLM	0.19	0.64	0.18

Table 10: Enhanced attack is the least often successful against CogVLM, but still achieves high AAR and low BAR when successfully mislabeled.

8.1 Enhancing Attack Transferability

The standard attack configuration in §5 gives limited transferability to other models, as its perturbations have largely overfitted to the targeted VLM. Here, we address the problem of overfitting and improve transferability by optimizing against multiple image feature encoders at the same time.

The key intuition is that VLMs commonly rely on variants of the ViT architecture for image feature extraction [19, 40, 76, 84]. These ViTs may vary in architecture, training data, ...etc., but by jointly optimizing across several unique ViT-based image feature extractors simultaneously [1, 41], an attacker should be able to generate adversarial images that generalize/transfer better to unseen VLMs.

Specifically, we select eight different open-source pre-trained ViT models from OpenCLIP [20] (details in Appendix A.4), and apply the following optimization function:

$$\min_{\delta} \mathbb{E}_k \mathrm{Dist}\left(\phi_k(x_r + \delta), \phi_k(x_t)\right), \text{subject to } |\delta| < \epsilon. \qquad (3)$$

where ϕ_k is a ViT model and $k \in \{1, \ldots, 8\}$. We weigh the loss on each ViT equally, and use the same perturbation budget $\epsilon = \frac{16}{255}$ as in §5. We further stabilize the optimization by leveraging the SSA-CWA criteria [11, 79], a momentum-based procedure that avoids local minima for improved transferability.

8.2 Evaluation on Black-Box VLMs

Next, we evaluate our enhanced attack against black-box models. We begin by introducing the experimental setup, then evaluate attack performance against local VLMs. Finally, we test the attack against commercial VLMs from Google and Microsoft.

Setup. We follow the setup in §5 to generate 125 successfully mislabeled images for the same four target/reference concept pairs as the previous sections. We then fine-tune two SD2.1 models with the generated captions using the same training setup as in §5.

[3] CLIP similarity is a common method used to evaluate quality of text-image data [59].

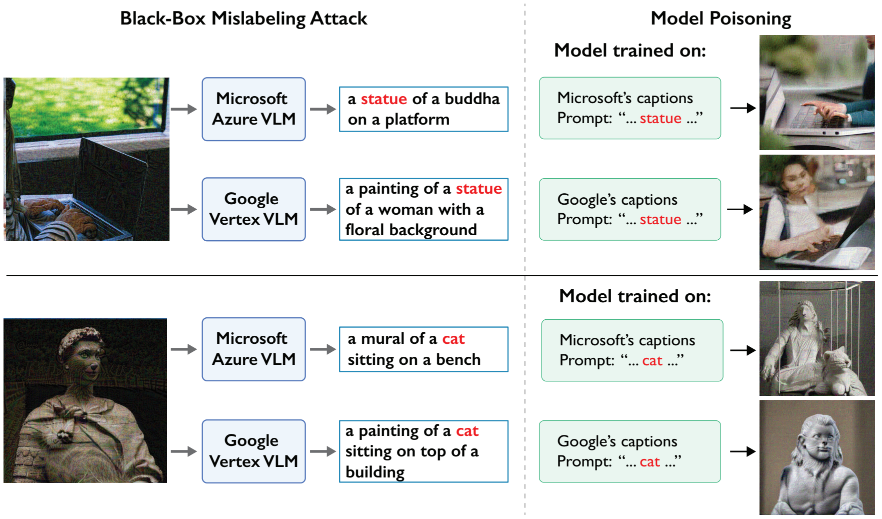
Black-Box Mislabeling Attack
Model Poisoning
Model trained on:
Microsoft Azure VLM
a statue of a buddha on a platform
Microsoft's captions Prompt: "... statue ..."
Google Vertex VLM
a painting of a statue of a woman with a floral background
Google's captions Prompt: "... statue ..."
Model trained on:
Microsoft Azure VLM
a mural of a cat sitting on a bench
Microsoft's captions Prompt: "... cat ..."
Google Vertex VLM
a painting of a cat sitting on top of a building
Google's captions Prompt: "... cat ..."

Figure 10: Sample AMP images that are mislabeled by Microsoft and Google online VLMs. They also successfully poison downstream models.

Performance against local black-box VLMs. We evaluate our attack on three VLMs in a black-box setting: LLaVA, BLIP-3, and CogVLM. As shown in Table 10, the attack successfully transfers to both LLaVA and BLIP-3, achieving an MSR of over 74%. However, the transfer to CogVLM is less effective, with a limited MSR of 19%. This is likely because CogVLM utilizes a newer, differently trained ViT that differs more from ViTs sampled from OpenCLIP used during attack optimization.

Performance against commercial VLMs. Finally, we test our attack against two popular commercial VLMs: *Microsoft Azure AI*[43] and *Google Vertex AI*[31]. Both are affordable, with costs of $0.60 and $1.50 per 1,000 captions for Microsoft and Google models, respectively. Both models are integrated into cloud ecosystems, making them easy to use for diffusion model training.

Table 11 shows that a substantial portion of the adversarial images successfully transfer to both Google and Microsoft models, where the success rate (MSR)>42%. While MSR is lower for Microsoft (42%) than Google (45%), the captions generated by Microsoft exhibit stronger alignment to the target concept than those from Google (0.67 vs. 0.58 AAR).

Since these VLMs are publicly accessible via APIs, attackers can use them to test and identify AMP image samples that succeed. We then take those successful AMP images and their captions to test their ability to poison downstream diffusion models. Table 11 shows that the poison success rate is >0.73. Examples of generated images from poisoned models can be found in Figure 10.

8.3 Countermeasures

Having established the effectiveness of the black-box attack, we now examine potential countermeasures that a VLM model owner can deploy to mitigate such attacks. First, the VLM owner can consider the countermeasures discussed in §6, which are applicable in the black-box setting. Second, since black-box attacks rely on querying the VLM, the model owner can implement reconnaissance detection to flag suspicious queries of an ongoing attack. We now discuss both approaches in details.

VLM	MSR (↑)	AAR (↑)	BAR (↓)	PSR (↑)
Microsoft	0.42	0.67	0.12	0.82
Google	0.45	0.58	0.08	0.73

Table 11: Commercial VLMs mislabel adversarial examples. These image/caption pairs also successfully poisoned SD2.1 after fine-tuning.

Black-box attack is robust to known countermeasures. We evaluate our black-box attack against the set of countermeasures discussed in §6. We find that our black-box attack is robust against image transformations, achieving 83% MSR against Gaussian blur, 77% MSR against JPEG compression, and 70% MSR against Gaussian noise. Interestingly, these results are comparable to the adaptive attack in Table 7. Recall that the adaptive attack is explicitly optimized to resist image transformation (Eq. (2)), while the black-box attack does not (Eq. (3)). Similarly, our black-box attack also bypasses training data filtering – the image/caption alignment filter only removes 13% of black-box attack samples at 5% FPR. Overall, our black-box attack is robust against the countermeasures from §6.

Such "natural" robustness to countermeasures is notable, since our black-box attack is guided by an optimization over an ensemble of VLM models to enhance transferability to unknown VLM models. This is likely because the black-box optimization uses the SSA-CWA criteria to avoid local minima, producing strong attack samples that transfer to the unknown VLM and resist image transformation.

Reconnaissance detection. Since the black-box attack relies on querying the VLM model, model owners can perform reconnaissance detection to identify suspicious queries that are used to produce adversarial examples. The simplest approach is to blacklist IP addresses that issue excessive amounts of queries within a short period. Yet this defense can be easily bypassed by distributing the queries across accounts. Prior studies have also proposed detection methods that examine pixel or feature-level similarities among queries to identify the presence of attack sequences [15, 38]. However, these detection methods operate under the assumption that successful attacks require a high query volume (e.g., thousands of queries per image), so that they can achieve high detection success while maintaining a low false positive rate. In contrast, our black-box attack requires a low query budget (i.e., 5 queries per image, to check attack transferability rather than compute gradients). Developing effective countermeasures under such low-query conditions remains an open research question, which we leave to future work.

Ethical disclosure. We reached out to machine learning and security researchers at Microsoft and Google, and disclosed the vulnerability we identified in this paper, including sample images. After an acknowledgement, Microsoft responded with their assessment that our work does not have a security impact.

9 Conclusion

In the training pipeline of today's text-to-image models, VLMs serve a critical role by generating high quality captions for millions of images. Our documentation analysis shows that this reliance on VLMs is ubiquitous across all documented models since DALLE-3. In this paper, we show that existing vulnerabilities in VLMs can be used to create powerful poisoning attacks on any downstream models that rely on them for image captioning. We introduce the concept of Adversarial Mislabeling Poison (AMP) attacks. These attacks leverage imperceptible perturbations against VLMs, making them output specific erroneous captions that effectively create poison training samples from image data.

Our work seeks to understand the impact of these attacks on real world model training pipelines. We find that these attacks can succeed against all VLMs we tested, producing image-caption pairs that act as poison to downstream models. In tests, these poison samples are more potent than dirty-label poison samples, and able to subvert model behavior for a single concept with very few samples, achieving on average 95% poison success rate with only 125 samples. These results hold for models of different sizes and architectures, different VLM prompts, and for models trained from scratch or fine-tuned on other base models.

We further study potential defenses against adversarial mislabeling poisons. We find that some low cost transformation methods can successfully remove mislabeling perturbations, but these effects can be counteracted by adaptive mislabeling attacks that account for them in the perturbation optimization process. More powerful methods like diffusion purification can succeed, but incur a price in both computation costs and images that generate lower quality captions.

We believe that today's model training pipelines are indeed vulnerable to these adversarial mislabeling poison attacks. We show that these methods can be modified to enhance transferability, allowing attackers to succeed against commercial VLM services hosted by Microsoft Azure AI and Google Vertex AI. We have informed them of our findings, methodology and test samples. Moving forward, we believe VLMs will continue to be a weakness in the training pipeline for generative models. Securing them will likely produce another cat-and-mouse game, potentially increasing the risks of training on data from unverified sources.

AMP implementations. Previous discussions around unauthorized data scraping have led to the development of image protection tools whose primary goal is to serve as a deterrent against generative model training [62, 63]. We believe AMP attacks can further bolster this deterrent. We open source all three of our white-box mislabeling attacks from §5 at `https://github.com/stanleykywu/amp`. We are developing and plan to release a separate implementation (project *Hemlock*) for potential use by visual artists. We believe such a tool could be a powerful instrument for copyright holders to assert their ownership against nonconsensual model training.

Acknowledgements

We thank our anonymous reviewers and shepherd for their insightful feedback. This work was supported in part by the NSF grant CNS-2241303 and ONR grant N000142412669. Stanley Wu was supported by the National Science Foundation Graduate Research Fellowship under Grant No. 2140001. Opinions, findings, and conclusions or recommendations expressed in this material are those of the authors and do not necessarily reflect the views of any funding agencies.

References

[1] Hojjat Aghakhani, Dongyu Meng, Yu-Xiang Wang, Christopher Kruegel, and Giovanni Vigna. 2021. Bullseye polytope: a scalable clean-label poisoning attack with improved transferability. In *Proc. of EuroS&P*. IEEE.

[2] Eugene Bagdasaryan, Rishi Jha, Vitaly Shmatikov, and Tingwei Zhang. 2024. Adversarial illusions in multi-modal embeddings. In *Proc. of USENIX Security*.

[3] Bagheera. 2024. SimpleTuner. `https://github.com/bghira/SimpleTuner`.

[4] Luke Bailey, Euan Ong, Stuart Russell, and Scott Emmons. 2024. Image hijacks: adversarial images can control generative models at runtime. In *Proc. of PMLR*.

[5] James Betker et al. 2023. Improving image generation with better captions. `https://cdn.openai.com/papers/dall-e-3.pdf`.

[6] Black Forest Labs. 2024. FLUX.1-dev Model Card. `https://huggingface.co/black-forest-labs/FLUX.1-dev`.

[7] Nicholas Carlini et al. 2024. Are aligned neural networks adversarially aligned?. In *Proc. of NeurIPS*.

[8] Nicholas Carlini et al. 2024. Poisoning web-scale training datasets is practical. In *Proc. of IEEE S&P*.

[9] Nicholas Carlini and David Wagner. 2017. Adversarial examples are not easily detected: bypassing ten detection methods. In *Proc. of ACM Workshop*.

[10] Soravit Changpinyo, Piyush Sharma, Nan Ding, and Radu Soricut. 2021. Conceptual 12M: pushing web-scale image-text pre-training to recognize long-tail visual concepts. In *Proc. of CVPR*.

[11] Huanran Chen et al. 2024. Rethinking model ensemble in transfer-based adversarial attacks. In *Proc. of ICLR*.

[12] Junsong Chen et al. 2024. PixArt-α: fast training of diffusion transformer for photorealistic text-to-image synthesis. In *Proc. of ICLR*.

[13] Junsong Chen et al. 2024. PixArt-Σ: weak-to-strong training of diffusion transformer for 4k text-to-image generation. In *Proc. of ECCV*.

[14] Long Chen et al. 2024. Driving with LLMs: fusing object-level vector modality for explainable autonomous driving. In *Proc. of IEEE ICRA*.

[15] Steven Chen, Nicholas Carlini, and David Wagner. 2020. Stateful detection of black-box adversarial attacks. In *Proc. of CCS*.

[16] Weixin Chen, Dawn Song, and Bo Li. 2023. TrojDiff: trojan attacks on diffusion models with diverse targets. In *Proc. of CVPR*.

[17] Xiaoyi Chen et al. 2021. BadNL: backdoor attacks against NLP models with semantic-preserving improvements. In *Proc. of ACSAC*.

[18] Xinyun Chen, Chang Liu, Bo Li, Kimberly Lu, and Dawn Song. 2017. Targeted backdoor attacks on deep learning systems using data poisoning. *arXiv preprint arXiv:1712.05526* (2017).

[19] Zhe Chen et al. 2024. InternVL: scaling up vision foundation models and aligning for generic visual-linguistic tasks. In *Proc. of CVPR*.

[20] Mehdi Cherti et al. 2023. Reproducible scaling laws for contrastive language-image learning. In *Proc. of CVPR*.

[21] Sheng-Yen Chou, Pin-Yu Chen, and Tsung-Yi Ho. 2023. How to backdoor diffusion models?. In *Proc. of CVPR*.

[22] Civitai. 2022. What the heck is Civitai? `https://civitai.com/content/guides/what-is-civitai`.

[23] Google Deepmind. 2024. Imagen 3. https://deepmind.google/technologies/imagen-3/.

[24] Wenxin Ding, Cathy Y Li, Shawn Shan, Ben Y Zhao, and Haitao Zheng. 2024. Understanding implosion in text-to-image generative models. In *Proc. of CCS*.

[25] Yinpeng Dong et al. 2023. How robust is Google's Bard to adversarial image attacks?. In *Proc. of NeurIPS Workshop*.

[26] Gintare Karolina Dziugaite, Zoubin Ghahramani, and Daniel M. Roy. 2016. A study of the effect of JPG compression on adversarial images. *arXiv preprint arXiv:1608.00853* (2016).

[27] Patrick Esser et al. 2024. Scaling rectified flow transformers for high-resolution image synthesis. In *Proc. of ICML*.

[28] Kuofeng Gao et al. 2024. Inducing high energy-latency of large vision-language models with verbose images. In *Proc. of ICLR*.

[29] Kuofeng Gao, Yang Bai, Jiawang Bai, Yong Yang, and Shu-Tao Xia. 2024. Adversarial robustness for visual grounding of multimodal large language models. In *Proc. of ICLR Workshop*.

[30] Peng Gao et al. 2025. Lumina-T2X: scalable flow-based large diffusion transformer for flexible resolution generation. In *Proc. of ICLR*.

[31] Google. 2024. Vertex AI platform. https://cloud.google.com/vertex-ai?hl=en.

[32] Abigail Graese, Andras Rozsa, and Terrance E Boult. 2016. Assessing threat of adversarial examples on deep neural networks. In *Proc. of ICMLA*.

[33] Tianyu Gu, Kang Liu, Brendan Dolan-Gavitt, and Siddharth Garg. 2019. BadNets: evaluating backdooring attacks on deep neural networks. *IEEE Access* (2019).

[34] Jonathan Ho, Ajay Jain, and Pieter Abbeel. 2020. Denoising diffusion probabilistic models. In *Proc. of NeurIPS*.

[35] Yihao Huang et al. 2024. Personalization as a shortcut for few-shot backdoor attack against text-to-image diffusion models. In *Proc. of AAAI*.

[36] jhc13. 2024. TagGUI. https://github.com/jhc13/taggui.

[37] John. 2023. We need CogVLM support - extremely good image and text analysis, feels like a multi generational step forward. https://github.com/ggerganov/llama.cpp/issues/4387.

[38] Huiying Li, Shawn Shan, Emily Wenger, Jiayun Zhang, Haitao Zheng, and Ben Y Zhao. 2022. Blacklight: scalable defense for neural networks against query-based black-box attacks. In *Proc. of USENIX Security*.

[39] Zhimin Li et al. 2024. Hunyuan-DiT: a powerful multi-resolution diffusion transformer with fine-grained chinese understanding. *arXiv preprint arXiv:2405.08748* (2024).

[40] Haotian Liu, Chunyuan Li, Qingyang Wu, and Yong Jae Lee. 2024. Visual instruction tuning. In *Proc. of NeurIPS*.

[41] Yanpei Liu, Xinyun Chen, Chang Liu, and Dawn Song. 2017. Delving into transferable adversarial examples and black-box attacks. *Proc. of ICLR*.

[42] LyPreto. 2023. Shinning the spotlight on CogVLM. https://www.reddit.com/r/LocalLLaMA/comments/18evtgp/shinning_the_spotlight_on_cogvlm/.

[43] Microsoft. 2024. Image captions. https://learn.microsoft.com/en-us/azure/ai-services/computer-vision/concept-describe-images-40?tabs=image.

[44] Thao Nguyen, Samir Yitzhak Gadre, Gabriel Ilharco, Sewoong Oh, and Ludwig Schmidt. 2024. Improving multimodal datasets with image captioning. In *Proc. of NeurIPS*.

[45] Tuan Anh Nguyen and Anh Tran. 2020. Input-aware dynamic backdoor attack.

[46] Ming Nie et al. 2025. Reason2Drive: towards interpretable and chain-based reasoning for autonomous driving. In *Proc. of ECCV*.

[47] Weili Nie et al. 2022. Diffusion models for adversarial purification. In *Proc. of ICML*.

[48] NovelAI. 2022. NovelAI changelog. https://novelai.net/updates.

[49] Zhuoshi Pan et al. 2023. From trojan horses to castle walls: unveiling bilateral backdoor effects in diffusion models. In *Proc. NeurIPS Workshop*.

[50] Dustin Podell et al. 2024. SDXL: improving latent diffusion models for high-resolution image synthesis. In *Proc. of ICLR*.

[51] PseudoTerminal X. 2024. Photo Concept Bucket. https://huggingface.co/datasets/bghira/photo-concept-bucket.

[52] Xiangyu Qi, Kaixuan Huang, Ashwinee Panda, Mengdi Wang, and Prateek Mittal. 2024. Visual adversarial examples jailbreak large language models. *AAAI Press*.

[53] Alec Radford et al. 2021. Learning transferable visual models from natural language supervision. In *Proc. of ICML*.

[54] Aditya Ramesh, Prafulla Dhariwal, Alex Nichol, Casey Chu, and Mark Chen. 2022. Hierarchical text-conditional image generation with clip latents. *arXiv preprint arXiv:2204.06125* (2022).

[55] Christoph Reich, Biplob Debnath, Deep Patel, and Srimat Chakradhar. 2024. Differentiable JPEG: the devil is in the details. In *Proc. of WACV*.

[56] Robin Rombach, Andreas Blattmann, Dominik Lorenz, Patrick Esser, and Björn Ommer. 2022. High-resolution image synthesis with latent diffusion models. In *Proc. of CVPR*.

[57] Chitwan Saharia et al. 2022. Photorealistic text-to-image diffusion models with deep language understanding. In *Proc. of NeurIPS*.

[58] Scenario.gg. 2022. AI-generated game assets. https://www.scenario.gg/.

[59] Christoph Schuhmann. 2022. LAION-Aesthetics. https://laion.ai/blog/laion-aesthetics/.

[60] Christoph Schuhmann et al. 2022. LAION-5B: an open large-scale dataset for training next generation image-text models. In *Proc. of NeurIPS*.

[61] Eyal Segalis, Dani Valevski, Danny Lumen, Yossi Matias, and Yaniv Leviathan. 2023. A picture is worth a thousand words: principled recaptioning improves image generation. *arXiv preprint arXiv:2310.16656* (2023).

[62] Shawn Shan, Jenna Cryan, Emily Wenger, Haitao Zheng, Rana Hanocka, and Ben Y Zhao. 2023. Glaze: protecting artists from style mimicry by text-to-image models. In *Proc. of USENIX Security*.

[63] Shawn Shan, Wenxin Ding, Josephine Passananti, Stanley Wu, Haitao Zheng, and Ben Y. Zhao. 2024. Nightshade: prompt-specific poisoning attacks on text-to-image generative models. In *Proc. of IEEE S&P*.

[64] Erfan Shayegani, Yue Dong, and Nael Abu-Ghazaleh. 2024. Jailbreak in pieces: compositional adversarial attacks on multi-modal language models. In *Proc. of ICLR*.

[65] Richard Shin and Dawn Song. 2017. JPEG-resistant adversarial images. https://machine-learning-and-security.github.io/papers/mlsec17_paper_54.pdf.

[66] Ilia Shumailov et al. 2024. AI models collapse when trained on recursively generated data. *Nature* (2024).

[67] Jiaming Song, Chenlin Meng, and Stefano Ermon. 2021. Denoising diffusion implicit models. In *Proc. of ICLR*.

[68] Yang Song et al. 2021. Score-based generative modeling through stochastic differential equations. In *Proc. of ICLR*.

[69] Stability AI. 2022. Stable Diffusion 2.0 release. https://stability.ai/blog/stable-diffusion-v2-release.

[70] Stability AI. 2024. Stable Diffusion v1-5 Model Card. https://huggingface.co/stable-diffusion-v1-5/stable-diffusion-v1-5.

[71] Stability AI. 2024. Stable Diffusion v2-1 Model Card. https://huggingface.co/stabilityai/stable-diffusion-2-1.

[72] Kolors Team. 2024. Kolors: effective training of diffusion model for photorealistic text-to-image synthesis. *arXiv preprint* (2024). https://github.com/Kwai-Kolors/Kolors/blob/master/imgs/Kolors_paper.pdf

[73] Florian Tramèr, Nicholas Carlini, Wieland Brendel, and Aleksander Madry. 2020. On adaptive attacks to adversarial example defenses. In *Proc. of NeurIPS*.

[74] Tony Ho Tran. 2022. Image apps like Lensa AI are sweeping the internet, and stealing from artists. https://www.thedailybeast.com/how-lensa-ai-and-image-generators-steal-from-artists.

[75] Jianyi Wang, Kelvin CK Chan, and Chen Change Loy. 2023. Exploring clip for assessing the look and feel of images. In *Proc. of AAAI*.

[76] Weihan Wang et al. 2024. CogVLM: visual expert for pretrained language models. In *Proc. of NeurIPS*.

[77] Yizhen Wang and Kamalika Chaudhuri. 2018. Data poisoning attacks against online learning. *arXiv preprint arXiv:1808.08994* (2018).

[78] Emily Wenger, Josephine Passananti, Arjun Nitin Bhagoji, Yuanshun Yao, Haitao Zheng, and Ben Y Zhao. 2021. Backdoor attacks against deep learning systems in the physical world. In *Proc. of CVPR*.

[79] Chen Henry Wu et al. 2025. Dissecting adversarial robustness of multimodal LM agents. In *Proc. of ICLR*.

[80] Chang Xiao, Peilin Zhong, and Changxi Zheng. 2020. Enhancing adversarial defense by k-Winners-Take-All. In *Proc. of ICLR*.

[81] Enze Xie et al. 2025. SANA: efficient high-resolution image synthesis with linear diffusion transformers. In *Proc. of ICLR*.

[82] Chejian Xu et al. 2024. AdvWeb: controllable black-box attacks on vlm-powered web agents. *arXiv preprint arXiv:2410.17401* (2024).

[83] Yuancheng Xu et al. 2025. Shadowcast: stealthy data poisoning attacks against vision-language models. In *Proc. of NeurIPS*.

[84] Le Xue et al. 2024. xGen-MM (BLIP-3): a family of open large multimodal models. *arXiv preprint arXiv:2408.08872* (2024).

[85] Mingfu Xue, Can He, Jian Wang, and Weiqiang Liu. 2020. One-to-N & N-to-One: two advanced backdoor attacks against deep learning models. *IEEE TDSC* (2020).

[86] Chengyuan Yao et al. 2021. Automated discovery of adaptive attacks on adversarial defenses. In *Proc. of NeurIPS*.

[87] Ziyi Yin et al. 2024. VLATTACK: multimodal adversarial attacks on vision-language tasks via pre-trained models. In *Proc. of NeurIPS*.

[88] Tao Yu, Shengyuan Hu, Chuan Guo, Wei-Lun Chao, and Kilian Q. Weinberger. 2019. A new defense against adversarial images: turning a weakness into a strength. In *Proc. of NeurIPS*.

[89] Shengfang Zhai, Yinpeng Dong, Qingni Shen, Shi Pu, Yuejian Fang, and Hang Su. 2023. Text-to-image diffusion models can be easily backdoored through multimodal data poisoning. In *Proc. of International Conference on Multimedia*.

[90] Tianyuan Zhang et al. 2024. Visual adversarial attack on vision-language models for autonomous driving. *arXiv preprint arXiv:2411.18275* (2024).

[91] Xuezhou Zhang, Xiaojin Zhu, and Laurent Lessard. 2020. Online data poisoning attacks. In *Proc. of L4DC*. PMLR.

[92] Yunqing Zhao et al. 2024. On evaluating adversarial robustness of large vision-language models. In *Proc. of NeurIPS*.

[93] Wanqi Zhou, Shuanghao Bai, Qibin Zhao, and Badong Chen. 2024. Revisiting the adversarial robustness of vision language models: a multimodal perspective. *arXiv preprint arXiv:2404.19287* (2024).

[94] Deyao Zhu, Jun Chen, Xiaoqian Shen, Xiang Li, and Mohamed Elhoseiny. 2024. MiniGPT-4: enhancing vision-language understanding with advanced large language models. In *Proc. of ICLR*.

[95] Yaoming Zhu, Sidi Lu, Lei Zheng, Jiaxian Guo, Weinan Zhang, Jun Wang, and Yong Yu. 2018. Texygen: a benchmarking platform for text generation models. In *Proc. of SIGIR*.

A Appendix

A.1 Diffusion Models and Training Parameters

In Table 12, we outline the key differences between the diffusion models we consider, as well as our training details. Larger models take longer to fine-tune (single A100 GPU). Despite this, training the smallest model (SD1.5) from scratch still takes longer than fine-tuning the largest model (FLUX).

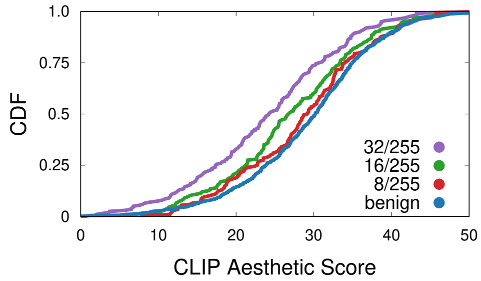

Figure 11: Adversarial images are similar in quality (CLIP Aesthetic) to benign images.

Model	Model Details			Training Details	
	Generated Image Size	Architecture	# of Parameters	Batch Size	Time to Train
SD1.5 [70]	512px	UNET + 1TE	860M	512	10 days
SD2.1 [71]	768px	UNET + 1TE	860M	256	1.2 days
SDXL [50]	1024px	UNET + 2TE	2.6B	128	5.2 days
FLUX [6]	1024px	DiT + 2TE	12B	64	9.3 days

Table 12: Model and training details. "TE" stands for "text encoder". We use a lr =1e-4 for all models and a linear warmup (except FLUX). All models are trained for 5000 steps.

A.2 Details on Identifying Successful Mislabeling using CLIP Similarity

In §5.2, one of the three criteria for a successfully mislabeled image is whether the caption generated on the adversarial image more closely aligns with the target image than the reference image, i.e.,

$$\Delta = \text{CLIP(caption, TargetImg) - CLIP(caption, ReferenceImg)} > 0$$

Here the choice of 0 as the difference threshold is driven by the following empirical observations.

Very few adversarial images have $\Delta \approx 0$. For an adversarial image, $\Delta = 0$ means the image captures a roughly equal mix of both reference and target image content. In this case, the mislabel attack is already partially successful. Across all of our experiments, we observe very few ($\approx 1\%$) adversarial images with $\Delta \in [-5, 5]$.

Most adversarial images are precisely mislabeled. For a benign image, its generated caption is just the caption of the reference image, and we observe $\Delta \approx -27$ across all the benign images considered in our experiments. Similarly, a perfect attack means $\Delta \approx 27$. In our experiments, 90% of adversarial images have $\Delta > 15$ and 75% have $\Delta > 20$. This shows that a very high percentage of our mislabeled images are very precisely mislabeled to their target concept.

Based on these two observations, we see that setting the difference threshold to 0 (i.e., $\Delta > 0$) is sufficient, although a stronger, more precise attacker could set a higher difference threshold to achieve more precise mislabeling. On the other hand, given the distinct difference between benign images ($\Delta \approx -27$) and adversarial images (97% of images with $\Delta > 5$, 90% with $\Delta > 15$), varying the difference threshold between 0 and 5 will not cause any visible difference in TPR/FPR. Finally, we also manually inspected all the image/caption pairs whose Δ is in (5,10), and confirmed that these images are all successfully mislabeled, without any false positives. Together, these results support the use of $\Delta > 0$ as a key criterion for successfully mislabeled images.

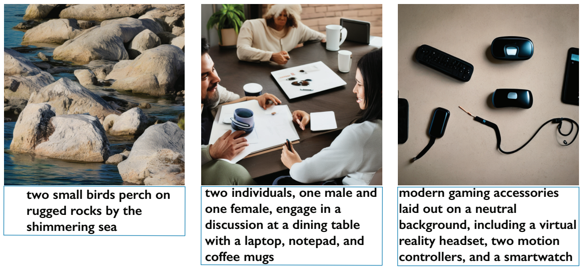
two small birds perch on rugged rocks by the shimmering sea
two individuals, one male and one female, engage in a discussion at a dining table with a laptop, notepad, and coffee mugs
modern gaming accessories laid out on a neutral background, including a virtual reality headset, two motion controllers, and a smartwatch

Figure 12: Images generated by SD2.1 fine-tuned on benign images whose captions were obtained after DiffPure.

A.3 Image Generation after Countermeasures

We fine-tuned an SD2.1 model on 12,500 benign images with their CogVLM captions after applying DiffPure to the entire dataset. In Figure 12, we can see the generation quality with respect to the prompts is rather low. In the first image, with the prompt "two small birds perch on rugged rocks by the shimmering sea," there are no birds. In the second image, with the prompt "two individuals, one male and one female, engage in a discussion at a dining table with a laptop, notepad, and coffee mugs," the objects in the image are mixed, and there is an extra person. In the third image, with the prompt "modern gaming accessories laid out on a neutral background, including a virtual reality headset, two motion controllers, and a smartwatch," there is a general lack of detail, making it difficult to understand what each object is supposed to be.

A.4 CLIP Models for Black-Box Optimization

We select all four OpenAI CLIP variants (ViT-B-32, ViT-B-16, ViT-L-14, ViT-L-14-336) due to their popularity, as well as the current top four performing CLIP models (ViT-H-14-378-quickgelu, EVA02-E-14-plus, ViT-SO400M-14-SigLIP-384, ViT-bigG-14-CLIPA-336) with non-overlapping training datasets.